Structural and optical characterization of ZnS nanoparticles co-doped with Ni^{2+} and Cu^{2+}

V. Venkatasubbaian[1], K. Thamizharasan[2], R.Mohan[3]* and N. Punitha[4]

[1] Department of Physics, S.B.K. College, Aruppukottai – 626113, India
[2] Department of Physics, Sir Theagaraya College, Chennai – 600 021, India
[3] Department of Physics, Surya School of Engineering and Technology, Vikiravandi – 605 652, India
[4] Department of Physics, St.Joseph's College of Engineering, Chennai – 600 119, India

Abstract : $Zn_{0.97-x}Cu_x Ni_{0.03}S$ (x = 0.00, 0.01, 0.02, 0.03, 0.04 and 0.05) nanoparticles were synthesized by the chemical precipitation method. Poly vinyl pyrrolidone (PVP) was used to passivate the surface of the particles. The effect of Cu co-dopant on the structural, morphological and optical properties is discussed on the basis of EDS, FESEM, FTIR, UV-Vis and Pl results. EDX spectra confirmed the presence of Ni and Cu were incorporated at the Zn sites in the cubic structure without disturbing the original ZnS cubic structure. The particle size estimated from XRD was in the range of ~3.5 nm to 5 nm. FTIR spectra studies indicated that PVP simply co-exists on the surface of the nanoparticles and acts as the capping agent preventing agglomeration of the nanoparticles. Optical absorption studies showed a blue – shift of the fundamental absorption edge with respect to that of bulk ZnS. Enhanced photoluminescence was observed with increasing Cu concentration upto 3 wt% and beyond this photoluminescence quenching was observed.
Keywords: Structural and optical characterization, ZnS nanoparticles co-doped,Ni^{2+} and Cu^{2+}.

Introduction

ZnS is the most common and widely studied II B – VI group semiconductor with the wide band gap energy of 3.6 eV at 300 K, because it is stable, inexpensive, and relatively nontoxic compared with other NCs such as CdS, CdSe[1,2]. Efforts have been made to modulate the band gap emission and make ZnS exhibit the excellent optical properties by doping various types of impurities like Mn, Cu, Fe and Cd[3-6].However, there are very few reports on the wurtzite ZnS:Ni^{2+} Nanocrystals for improving the luminescent properties, and the shape-controlled synthesis in this case. ZnS nanocrystals doped with optically active luminescence centers create new opportunities for luminescence study and application of nanometer – scale materials[7-9]. Transition metals and rare earth – metals activated ZnS nanoparticles form a new class of luminescent materials[10-12]. Therefore, photoluminescence (PL) and electroluminescence (EL) properties of nanometer – scale ZnS:Mn, ZnS:Cu, ZnS:Ag, ZnS:Ni, ZnS:Co and ZnS:Ce….. have been studied extensively[13-19]. The synthesis method in

this paper is also a general method that can potentially be extended to prepare other transition metal ions (e.g. Fe^{2+}, Cu^{2+}, Mn^{2+}) doped ZnS nanomaterials.

Experimental section

Chemicals

Zinc acetate dehydrate (Zn(CH3COO)2.2H2O), Nickel acetate (Ni(CH3COO)2), Cupper Acetate (Cu(CH3COO)2), Sodium sulphide (Na2S) are used as reagent and Poly vinyl pyrrolidone (PVP) as a capping agent. All chemicals were purchased from Merck India Limited and used as received without further purification.

Sample preparation

In a typical synthesis of co-doped ZnS nanoparticles, 25ml ethanolic solution of 0.02 M zinc acetate was mixed with 0.3 mM Ni acetate solution and stirred well. After that, 0.2 mM co-doping ion (copper acetate) was added to the above solution. Drop wise addition of 0.01M Na2S immediately formed a deep whitish solution of co-doped $ZnS:Ni^{2+},Cu^{2+}$. Obtained solution was stirred vigorously upto half an hour and then 0.01M solution of PVP was mixed to prevent the further growth of nanocrystals. Resulting white precipitate was centrifuged and washed with alcohol and double distilled water in sequence . Subsequently, the precipitate was dried at 80° C in vacuum oven, to obtain the $ZnS:Ni^{2+},Cu^{2+}$ nanoparticles in powder form. To understand the effect of co-doping, three different samples were also prepared using single dopant ions (Ni^{2+} and Cu^{2+}) and without doping. The whole reaction process was carried out at room temperature with constant stirring.

Instrumentation

To investigate the structural and optical properties, the samples were characterized by X-Ray Diffraction (XRD), Scanning Electron Microscopy (SEM), Energy Dispersive Analysis by X-ray (EDX), UV–vis absorption (UV–vis) spectrometer and Photoluminescence (PL) spectrometer. X-ray diffraction (XRD) patterns were obtained by RigakuD / max-2200 PC diffractometer operated at 40 kV/20m A using Cu K α radiation (wavelength 1.5406 ˚ A) in the range from 20 to 80° on 2θ scale. SEM experiment was performed on JEOL JSM-6301F system, using an accelerating voltage of 160 KV with magnification of X30K while EDX pattern was collected by FEI Quanta 200. Optical absorption measurements were carried out using Perkin ElmerLamda-35 UV–vis spectrometer ranging from 250 to 600 nm. PL spectra of the samples were recorded with Perkin Elmer LS-55 photolumi- nescence spectrophotometer with 305 nm excitation wavelength.

Results and discussion

Crystallinity, size and phase of particles were characterized by XRD as shown in Fig. 1. Peak positions indicate the formation of zinc blend crystal structure with three most preferred orientations [111], [220] and [311]. No observable impurity phases in the spectra, indicating the formation of pure cubic phase of ZnS only while broadening of the diffraction peaks show the formation of nano sized particles. The average nanocrystallite size are calculated from full width at half maximum (β) of XRD peaks using Debye–Scherrer's formula [20],

$$D = \frac{k\lambda}{\beta Cos\theta}$$

Where λ is the wavelength of incident X-ray (1.54 Å) and θ is the Bragg's angle. From the calculations, the average diameter of the particles is 2.82 ± 0.5 nm for undoped and ZnS: Ni 3% samples.

The substitution of the Zn^{2+} ions (r Zn $^{2+}$ = 0.78 Å) with the higher radius Ni^{2+} ions (r Ni^{2+} = 0.69 Å) and Cu^{2+} ions (r Cu^{2+} = 0.83 Å) results a small increase in lattice constant of ZnS. This increased lattice constant gives the strong evidence for the incorporation of dopant ion into the host matrix which is also confirmed by PL spectra.

Size and morphology of co-doped ZnS nanoparticles analyzed by SEM is represented in Fig. 2. Image reveals that the nano- crystals are spherical in shape with smooth surface (> 100 nm), which is larger than the size estimated by the Scherrer formula calculations based on XRD pattern. Discrepancy between SEM and

XRD results divulge that prepared particles are polycrystalline in nature. In order to confirm the presence of Ni^{2+} and Cu^{2+} ions in the material, we perform the EDX study of co-doped sample. According to EDX spectra as shown in Fig. 3, it is clear that the final product contains strong atomic percentage of Zn (27.86%) and S (17.90%) as compared to Ni^{2+} and Cu^{2+} ions due to the small doping concentration. Additional signals like carbon and oxygen are showing the presence of capping agent (PVP)[21].
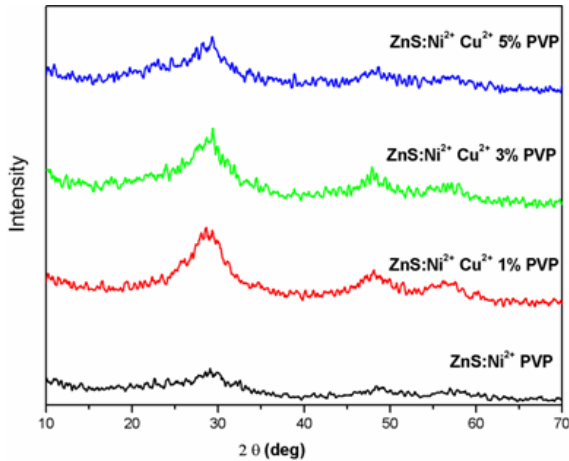

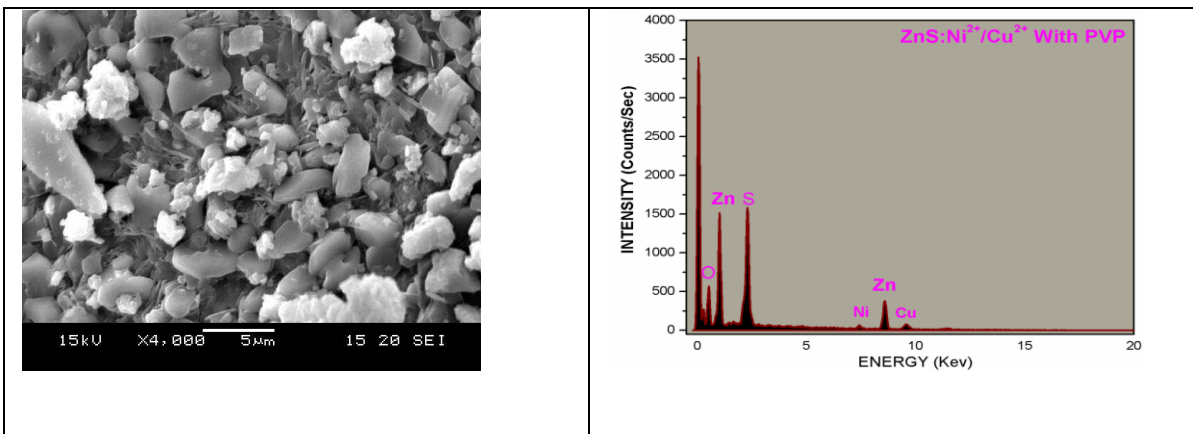**Fig.1. XRD diffraction patterns of doped and co-doped with ZnS nanoparticles**

Fig.2 FESEM image of co-doped with ZnS nanoparticles

Fig.3 EDX spectra of co-doped with ZnS nanoparticles

UV–vis absorption spectra of doped and co-doped samples along with the undoped sample are shown in the Fig. 4. Broad and less symmetric absorption peaks are observed at 295 nm that are effectively blue shifted as compared to the bulk bandgap wavelength (338 nm). It is clearly shown in Fig. 4 that the absorption edges are approximately same for all the samples and does not show any shifting with doping. This result may become due to effective small percentage of dopants. Blue shifting in excitonic absorption peak is attributed to the quantum size effect[22], where as the broadening and asymmetricity are due to the wide size distribution of synthesized particles as also shown in SEM results.
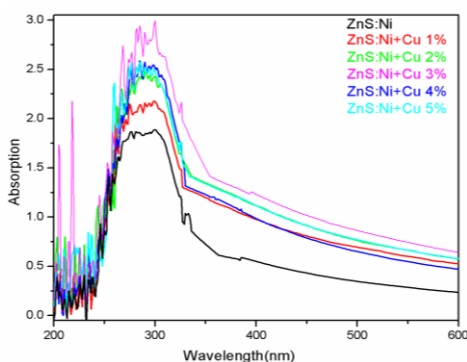

Fig.4 Absorption spectra of doped and co-doped with ZnS nanoparticles

Different size of particles give number of excitonic peaks that appear at different energies and overlapping of these peaks produces a broadening in absorption spectra[23]. It is well known that bandgap shifting in nano regime is based on the theoretical effective mass approximation model with the particle in a box approach and defined as [24,25.]

$$E_n = E_b + \left(\frac{h^2}{8R^2}\right)\left(\frac{1}{m_n} + \frac{1}{m_e}\right) - \frac{1.8e^2}{4\pi\varepsilon_o\varepsilon_r R}$$

Where r is the particle radius, e is the dielectric constant and m_e^* and m_h^* n are the effective masses of the electron and hole, respectively. First term in the above equation represents the kinetic energy of both electron and hole, second term corresponds to the Coulomb interaction and the last one is attributed to the correlation between two particles. For ZnS nanocrystals, the first order approximation gives the good relation between the particle radius (r) and bandgap (Eg) [26],Obtained value of particle size is about 2.5 nm using average band gap of 4.1 eV (295 nm) for all the spectra and it matches well with the values obtained from XRD.

Fourier transform infrared spectra (FTIR) is a versatile technique and gives detailed information about the chemical bonding and the elemental constituents of a material. Fig. 5 shows FTIR spectra of $Zn_{0.97-x}Ni_{0.03}Cu_xS$ (x=0.00, 0.02, 0.04, 0.06, 0.08 and 0.10) nanoparticles. The broad absorption peak around 3445 cm^{-1} is attributed to normal polymeric O–H stretching vibration of H_2O in ZnS:(Ni^{2+},Cu^{2+}) lattice because all FTIR spectra are recorded by mixing samples with KBr, which is hygroscopic.
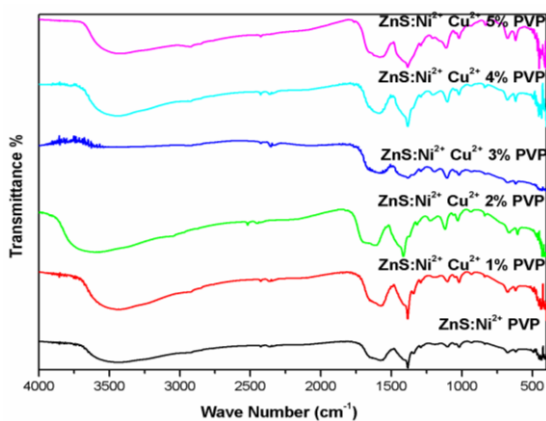

Fig.5 FTIR spectra of doped and co-doped with ZnS nanoparticles

The spectral band located at 2352cm^{-1} is related to N–H^{3+} stretching vibration of the amine group. The most intense bands at 1576cm^{-1} and 1384 cm^{-1} are the asymmetric and symmetric stretches of the coordinated PVP polymer[27]. However, the bands at1576 cm^{-1} and 1384 cm^{-1} indicate that the PVP are active in the ZnS:(Ni,Cu) matrices. The spectral band at 1100 cm^{-1} is attributed to C– O stretching related to ZnS:(Ni.Cu)–PVP [28]. The spectral bands at 676 and 478 cm^{-1} are assigned to the Zn–S stretching vibrations[29]. These IR spectra strongly support that the surface capping of the ZnS nanoparticles is by direct bonding of the PVP, to the ZnS site at the surface and does not interact chemically. This implies that PVP simply co-exists with the surface of the nanoparticles and acts as surfactant and prevents the agglomeration of the nanoparticles.

The excitation spectra of ZnS:Ni^{2+} and ZnS:(Ni^{2+},Cu^{2+}) nano-particles in the wavelength range of 250–600 nm shown in Fig. 6 indicate excitation maximum at 295 nm. The excitation spectrum of the ZnS:Ni^{2+} nanoparticles is considerably broadened compared to those of ZnS:(Ni^{2+},Cu^{2+}) nanoparticles. This broadening is mainly due to the strongly disordered surface which generates an individual random potential in each nanoparticle. This random potential induces enhanced fluctuations in the energy levels between different nanoparticles. The fluctuations of the levels increase with decreasing size of the particles, i.e., the excitation spectra broaden with decreasing and a very broad deep level emission band in the range of 350– 600 nm. It is seen that Cu^{2+}-doped ZnS samples exhibit three emission bands at 426, 486 and 538 nm. The peak at 426 nm is assigned to interstitial sulfur, where as the peak at 445 nm is assigned to zinc interstitial since sulfur ion has larger ionic radius (1.7 Å) than that of zinc ion (0.74 Å), interstitial sulfur produces more strain in the ZnS lattice and thus the electron levels due to this site will have smaller binding energy. So, the intense peak at 538 nm in sample A and C corresponds to the transition from Cu ions related defect states present in between the band gap.
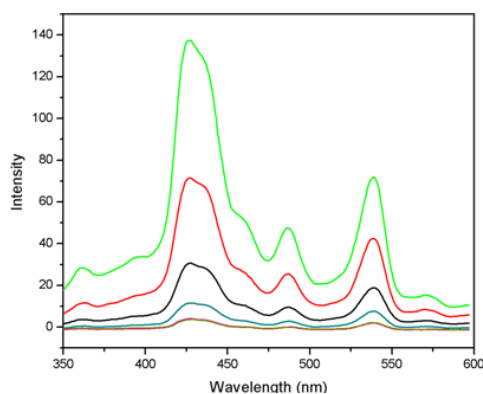
Fig.6 Pl spectra of doped and co-doped with ZnS nanoparticles

      The emission appearing in the blue region of the visible spectrum can be ascribed to a self-activated center presumably formed between a Zn vacancy and as hallow donor associated with a sulfur vacancy[30-32]. Sulfur vacancies at the surface are expected to give rise to Zn dangling bonds that form shallow donor levels. Thus, the recombination is mainly between these shallow donor levels and the valence band arising from a very fast energy transfer from the electron hole pair excited across the bandgap of the nanocrystals. In ZnS:(Ni^{2+},Cu^{2+}) samples an increase in emission intensity with Ni^{2+} content is noticed, with the PL peaks lightly shifted to 426 nm. The PL at 426 nm may be due to these. if activated luminescence, with the incorporation of Cu^{2+} into ZnS structure that resulted from the donor–acceptor pair (DAP) transition. Nagamani[33] also reported similar type of emission in Cu^{2+} doped ZnS nanoparticles formed by the solution growth method. This provides an obvious evidence for the entry of copper in host lattice. Although the emission spectra of Cu^{2+} co-doped samples appear similar, an appreciable luminescence enhancement was observed in Cu^{2+} co-doped samples compared to the ZnS: Ni^{2+} samples. The enhanced emission upon Cu^{2+} doping can be attributed to several factors such as (i) it is obvious that Cu^{2+} is acting as a sensitizing agent enhancing the radiative recombination processes. Thus, the photoluminescence efficiencies of ZnS:(Ni^{2+},Cu^{2+}) samples are higher than those of ZnS:Ni^{2+} samples. (ii) Increase of electron population in conduction band with doping of donor impurities. (iii) Higher rate of donor bound excitonic recombination (iv) and also sulfur vacancies are dominant in our samples with more sulfur vacancies being produced by the introduction of Cu^{2+}. All these factors might have enhanced the probability of enhanced of luminescence. Such anomalous intensity variation in Cu^{2+} codoped ZnS:Ni^{2+} nanoparticles can be understood considering the possibility of Cu^{2+} entering at interstitial sites. While for low doping concentrations 1–3 at% most of the Cu^{2+} ions might have been incorporated into the ZnS lattice through substitution, for higher concentrations, the excess amount of Cu^{2+} ions might have been incorporated into the nanoparticles interstitially, the interstitially doped Cu^{2+} atoms creating larger amount of lattice defects. Hence at higher concentrations of Cu^{2+} doping the photoluminescence intensity decreases.

      The action of Zn^{2+}, Ni^{2+} and Cu^{2+} will continuously happen with progress of the precipitation reaction. The luminescence mechanism of ZnS nanoparticles co-doped with Ni^{2+} and Cu^{2+} can be described as follows: the nano sized ZnS matrix absorbs ultraviolet photons, the electrons are excited from the valence band to the conduction band and are trapped by defects. The recombination of the defects and the excitation states induced by the composite center of Ni^{2+} and Cu^{2+} occurs and visible light emission is observed. When Ni^{2+} and Cu^{2+} as activation ions are doped in ZnS nano-particles, more electrons are easily excited. And the radiative recombination of luminescence processes is enhanced. Thus, the relative fluorescence intensity of the co-doped samples is remarkably increased. Because the localized energy level of excitation states of the composite center of Ni^{2+} and Cu^{2+} varies with changing impurity mole ratios of Ni^{2+} and Cu^{2+} in ZnS nano-crystallites, the emission spectra of ZnS nanocrystallites co-doped with Ni^{2+} and Cu^{2+} are varied.

4. Conclusion

      Ni^{2+} and Cu^{2+} co-doped ZnS nanoparticles are successfully synthesized by chemical precipitation method. XRD, SEM analysis and absorption spectra confirm the formation of nanoparticles with size is found to be 2.82 ± 0.5 nm. EDS, XRD and FTIR studies reveal that Ni^{2+} and Cu^{2+} are incorporated into the ZnS host lattice without altering the crystal structure. With Cu^{2+} co-doping, the bandgap varied in the range of 4.05–3.95 eV. Enhanced photo luminescence with increase in Cu^{2+} co-doping was observed up to 3 at % and beyond 3 at% luminescence quenching was observed. FTIR spectra indicate that the PVP simply co-exists on the surface

of nanostructures and acts as a capping agent and inhibits the agglomeration of the nanoparticles.

References

1.   Sun. Q., Andrew. W., Li. L., Wang. D., Zhu. T., Xu. J., Yang. C., Li. Y., Nat. Photonics 1 (2007) 717.
2.   Fang. X., Adv. Mater. 21 (2009) 2034.
3.   Murugadoss, G. Lumin. J. 132 (2012) 2043.
4.   Kang. T., Sung. J., Shim. W., Moon. H., Cho. J., Jo. Y., Lee. W., Kim. B., J. Phys. Chem. C 113 (2009) 5352.
5.   Li. Y., Cao. C., Chen. Z., Chem. Phys. Lett. 55 (2011) 517.
6.   Geng. B., Zhang. L., Wang. G., Xie. T., Zhang. Y., Meng. G., Appl. Phys. Lett. 84 (2004) 2157.
7.   Li. Y., Ding. Y., Zhang. Y., Qian. Y., J. Phys. Chem. Solids 60   (1999) 13.
8.   Alivisatos. A.P., Science 271 (1996) 933.
9.   Bhargava. R.N., Gallagher. D., Welker. T., J. Lumin. 60 (1994) 275.
10. Yu. J., Liu. H., Wang. Y., Jia. W.Y., J. Lumin. 79 (1998) 191.
11. Yu. I., Senna. M., Appl. Phys. Lett. 66 (4) (1995) 424. [12].
12. Khosravi. A.A., AngelKundu. M., Jatwa. L., Deshpande. S.K., Appl. Phys. Lett. 67 (1995) 2702.
13. Diaz-Torres. L.A., Garcia. O.B., Struck. C.W., McFarlane. R.A., J. Lumin. 78 (1998) 69.
14. Papakonstantinou. D.D., Huang. J., Lianos. P., J. Mater. Sci. Lett. 17 (1998) 1571.
15. Bhargava. R.N., Gallagher. D., Hong. X., Nurmikko. A., Phys. Rev. Lett. 72 (1994) 416.
16. Khosravi. A.A., Kundu. M., Jatwa. L., Deshpande. S.K., Appl. Phys. Lett. 67 (1995) 2702.
17. Murase. N., Jagannathan. R., Kanematsu. Y., Watanabe. M., Kurita. A., Hirata. K., Yazawa. T., Kushida. T., J. Phys. Chem. B 103   (1999) 754.
18. Yang. P., Li. M.K., Xu. D., Yuan. D., Chang. J., Zhou. G., Pan. M.. Appl. Phys. A 73 (2001) 455.
19. Yang. P., Lu. M.K., Xu. D., Yuan. D., C. Song. C., Zhou. G., J. Phys. Chem. Solids 62 (2001) 1181.
20. Cullity. B.D., in: Elements of X-ray Diffraction, Addison-Wesley, Reading, MA, 1978.
21. Monika Mall and Lokendra Kumar, J. Lumin 130 (2010) 660.
22. Becker. W.G., Bard. A.J., J. Phys. Chem. 87 (1983) 4888.
23. Rao. C.N.R., Muller. A., Cheetham. A.K., The Chemistry of Nanomaterials, 2, Willey-VCH, New York, 2004.
24. Lippens. P.E., Lannoo. M., Phys. Rev. B 39 (1989) 10935.
25. Brus. L.E., J. Phys. Chem. 90 (1986) 2555.
26. Suyver. J.F., Wuister. S.F., Kelly. J.J., Meijerink. A., Nano Lett. 1 (2001) 8.
27. Krishna Kanta Haldar, Amitava Patra, Applied Physics Letters 95 (2009) 063103.
28. Amaranatha Reddy. D., Murali, G. Vijayalakshmi. R.P., Reddy. B.K., Applied Physics A 105 (2011)119.
29. Maged El-Kemary, Hany El-Shamy, Journal of Photochemistry and Photobiology 205 (2009) 151.
30. Amaranatha Reddy. D., Murali. G., Vijayalakshmi. R.P.,.Reddy. B.K, and Sreedhar. B.,Crystal Research and Technology 46 (2011) 731.
31. Reddy. D., Murali. G, Poornaprakash. B., Vijayalakshmi. R.P., Reddy. B. K., Applied Surface Science 258 (2012) 5206.
32. D. Amaranatha Reddy, S.Sambasivam, G.Murali, B.Poornaprakash, R.P. Vijayalakshmi, Y.Aparna, B.K.Reddy, and J.L.Rao, Journal of Alloys and Compounds 537 (2012) 208.
33. K. Nagamani, N.Revathi, P.Prathap, Y.Lingappa, K.T. Ramakrishna Reddy, Current Applied Physics 12 (2012) 380.

✲✲✲✲✲